Seasonal variability of convectively coupled equatorial waves (CCEWs) in recent high-top CMIP5 models

Dzaki Zakaria[1], Sandro W. Lubis[2] and Sonni Setiawan[1]
[1] Department of Geophysics and Meteorology, Bogor Agricultural University (IPB), Indonesia
[2] Department of Geophysical Sciences, The University of Chicago, USA

E-mail: dzakizakaria28@gmail.com

Abstract. Tropical weather system is controlled by periodic atmospheric disturbances ranging from daily to subseasonal time scales. One of the most prominent atmospheric disturbances in the tropics is convectively coupled equatorial waves (CCEWs). CCEWs are excited by latent heating due to a large-scale convective system and have a significant influence on weather system. They include atmospheric equatorial Kelvin wave, Mixed Rossby Gravity (MRG) wave, Equatorial Rossby (ER) wave and Tropical Depression (TD-type) wave. In this study, we will evaluate the seasonal variability of CCEWs activity in nine high-top CMIP5 models, including their spatial distribution in the troposphere. Our results indicate that seasonal variability of Kelvin waves is well represented in MPI-ESM-LR and MPI-ESM-MR, with maximum activity occurring during boreal spring. The seasonal variability of MRG waves is well represented in CanESM2, HadGEM2-CC, IPSL-CM5A-LR and IPSL-CM5A-MR, with maximum activity observed during boreal summer. On the other hand, ER waves are well captured by IPSL-CM5A-LR and IPSL-CM5A-MR and maximize during boreal fall; while TD-type waves, with maximum activity observed during boreal summer, are well observed in CanESM2, HadGEM2-CC, IPSL-CM5A-LR and IPSL-CM5A-MR. Our results indicate that the skill of CMIP5 models in representing seasonal variability of CCEWs highly depends on the convective parameterization and the spatial or vertical resolution used by each model.

1. Introduction

Convectively coupled equatorial waves (CCEWs) are one of the most prominent atmospheric disturbances in the tropics. These disturbances substantially control the tropical weather system periodically from daily to subseasonal time scales [1-5]. CCEWs are generated by large-scale convection in the equatorial region around 20° N – 20° S [5–8]. They are including atmospheric Kelvin wave, MRG wave, n=0 ER wave and TD-type waves [9, 7]. Kelvin waves propagate eastward with a period of approximately 12 – 20 days and are influenced by El-Nino phenomenon [10]. MRG waves propagate westward with a period of approximately 4–5 days and are significantly influenced by La-Nina phenomenon [10]. TD-type and ER waves have similar characteristics as MRG. These waves propagate westward and have period of approximately 3–5 days for TD-type waves and approximately 10 – 48 days for ER waves. According to [2], MRG and TD-type waves have an important role to generate tropical cyclone in west northern Pacific (WNP). The CCEWs activity has a strong influence on the variability of tropical weather. Moreover, vertical propagation of CCEWs activity has a significant impact on the dynamical coupling between troposphere and stratosphere [3,11,9].

Previous studies have shown that CCEWs are not well simulated in general circulation models (GCMs) in the twentieth century experiment from the Coupled Model Intercomparison Project phase 3 of the World Climate Research Program (CMIP3) [15]. The biases in simulating CCEWs in these models are associated with the use of convection parameterization in each model. However, the representation of CCEW's seasonal variability in high-top CMIP5 model has remained elusive. Therefore, it is worth

investigating how the recent high-top CMIP5 models represent the CCEWs' variability and also to understand what causes the discrepancies among the model simulations. The purpose of this study is to examine the seasonal variability of CCEW activity in recent high-top CMIP5 models, with the main focus on their spatial distribution in the troposphere.

2. Data and Methods

2.1 Data

CCEWs activity was identified using daily-mean outgoing longwave radiation (OLR) from nine CMIP5 and NOAA reanalysis (observation) from January 1975 to December 2005 (~30 years). This study focused on the equatorial latitudinal bands, between 20° N – 20° S with resolution of 2.5° x 2.5°. The nine models from CMIP5 were chosen, including MPI-ESM-LR, MPI-ESM-MR, IPSL-CM5A-MR, IPSL-CM5A-LR, CanESM2, HadGEM2-CC, MIROC-ESM, MRI-CGCM3 and CMCC-CESM. These models have the same component and complexity (atmosphere, land surface, ocean and sea-ice), but with different spatial resolution [2]. They also used different convective parameterization.

2.2 Space Time Spectral Analysis (STSA)

The zonal propagation of CCEWs activity was analysed by using STSA technique similar to [5]. This method is used to elucidate the wave propagation as a function zonal wavenumber (k) and frequency (ω). A brief formulation can be expressed as follow:

$$x(\lambda, t) = \Sigma_k xk\,(\lambda, t) \tag{1}$$

$$x(\lambda, t) = Re\ \Sigma_{k,\omega}[W_{k,\omega} e^{i(kx+\omega)} + W_{k,-\omega} e^{i(kx+\omega)}] \tag{2}$$

$$x_k(\lambda, t) = \sum_k \quad \sum_{\pm\omega} W_{k,\pm\omega}\ \cos\left(k\lambda \pm \omega t + \varphi_{k,\pm\omega}\right) \tag{3}$$

In this study, we used a modified version of STSA analysis, in which the raw datasets were not partitioned into equatorial symmetric and anti-symmetric components (no symmetry constraints).

2.3 Spatial Distribution

This method is used to study the seasonal variation of CCEWs activity. We use Hovmoller technique in order to understand the seasonal variation of the filtered fields. First, the modelled OLR dataset were interpolated to the fixed horizontal grid (2.5° x 2.5°) as in the observed OLR dataset, by using a bilinear interpolation. Then we calculate the monthly variance as well as the seasonal variance in order to encapsulate the amplitude of the waves.

3. Results

Figure 1 shows the space-time spectra diagram of CCEWs activity based on OLR daily data from the observation. The different colours in the polygon of STSA diagram indicate the observed frequency-zonal wavenumber bands for the Kelvin wave (red), MRG wave (magenta), ER wave (cyan), TD-type wave (green) and MJO (blue). We can see from this diagram that Kelvin wave propagate eastward with a period of 2.5 – 17 days. On the other hand, both MRG wave and ER wave propagate westward with period of 2.2 – 3.6 and 10 – 48 days, respectively. TD-type wave propagate westward with a period of 2.5 – 5 days. These filter bands are used as a wave domain to isolate the spatial and seasonal variability of CCEWs in some high tops CMIP5 models. The results from the model simulations will be compared

to the observation, therefore, the analysis from the NOAA dataset is considered as a reference observed values.

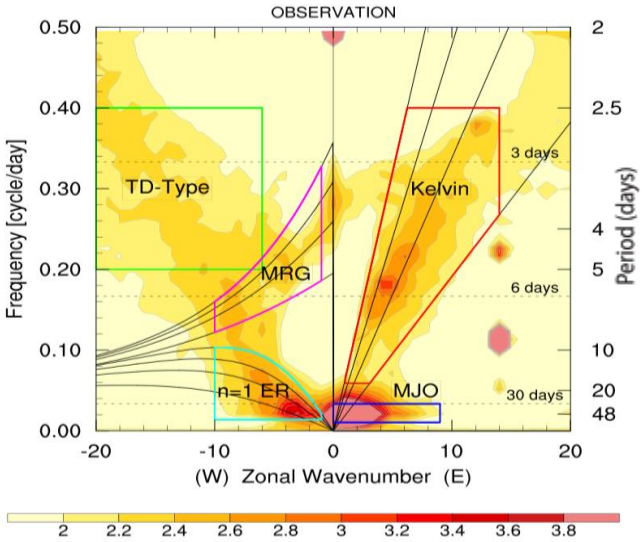

Figure 1. Zonal wavenumber frequency spectra of the anomalies OLR from observation (NOAA data reanalysis).

Figure 2 shows the seasonal evolution of Kelvin wave activity and its corresponding spatial distribution during JJA (June, July, August). We focus on JJA, since it is the season where the Kelvin wave activity is strongly observed in the observation and the model simulations. From the Hovmöller diagram, we can see that the observed Kelvin wave is strongly observed in the Northern Hemisphere (NH) equator (0-10^{o}N) from April to July, with amplitude around 120-160 (W/m^2)^2. The peak is observed in May (during boreal spring and summer). On ther other hand, in the Southern hemisphere (SH), the strongest activity is observed from June to December, with amplitude around 30-40 (W/m^2)^2 (Fig. 2, top). A seconadry active periode of Kelvin wave appears in October to November from boreal fall or early winter. Almost all CMIP5 models in Fig. 2, except MPI-ESM-LR and MPI-ESM-MR, unreasonably describe these main characteristics of the seasonal cycle. Nevertheless, both models underestimate the amplitude of the Kelvin waves in the equator. Other best candidates are CanESM2, HadGEM2-CC and MIROC-ESM, however the magnitude is still very low compared to that in the observation.

Figure 3 shows the seasonal evolution of MRG wave activity and its corresponding spatial distribution during JJA (June, July, August). Similar to Kelvin waves, we focus on JJA since it is the season where the MRG wave activity is strongly observed in both observation and model simulations. The results show that the MRG wave is strongly observed in the NH equator (0-10^{o}N) from December to April, with amplitude around 50-60 (W/m^2)^2. The peak is observed from June to August (JJA). In the SH, the MRG activity maximizes from April to January, however the amplitude is somewhat weaker compared to that in the NH, around 30-40 (W/m^2)^2. The best models that can simulate the seasonal cycle of MRG waves close to the observation are IPSL, CanESM2 and HandGEM2-CC.The observed MRG waves are stronger during JJA over the Northern Pacific to the Northern Atlantic, and they persists from May to December around with amplitude about 50–60 (W/m^2)^2 (Fig. 3). The IPSL, CanESM2 and HandGEM2-CC models are relatively good in representing the spatial distribution of MRG waves, however

the magnitudes are underrepresented (negative bias) over the northern part of the Pacific Ocean around 10 N and are overrepresented in the off-equatorial regions, around 20N.

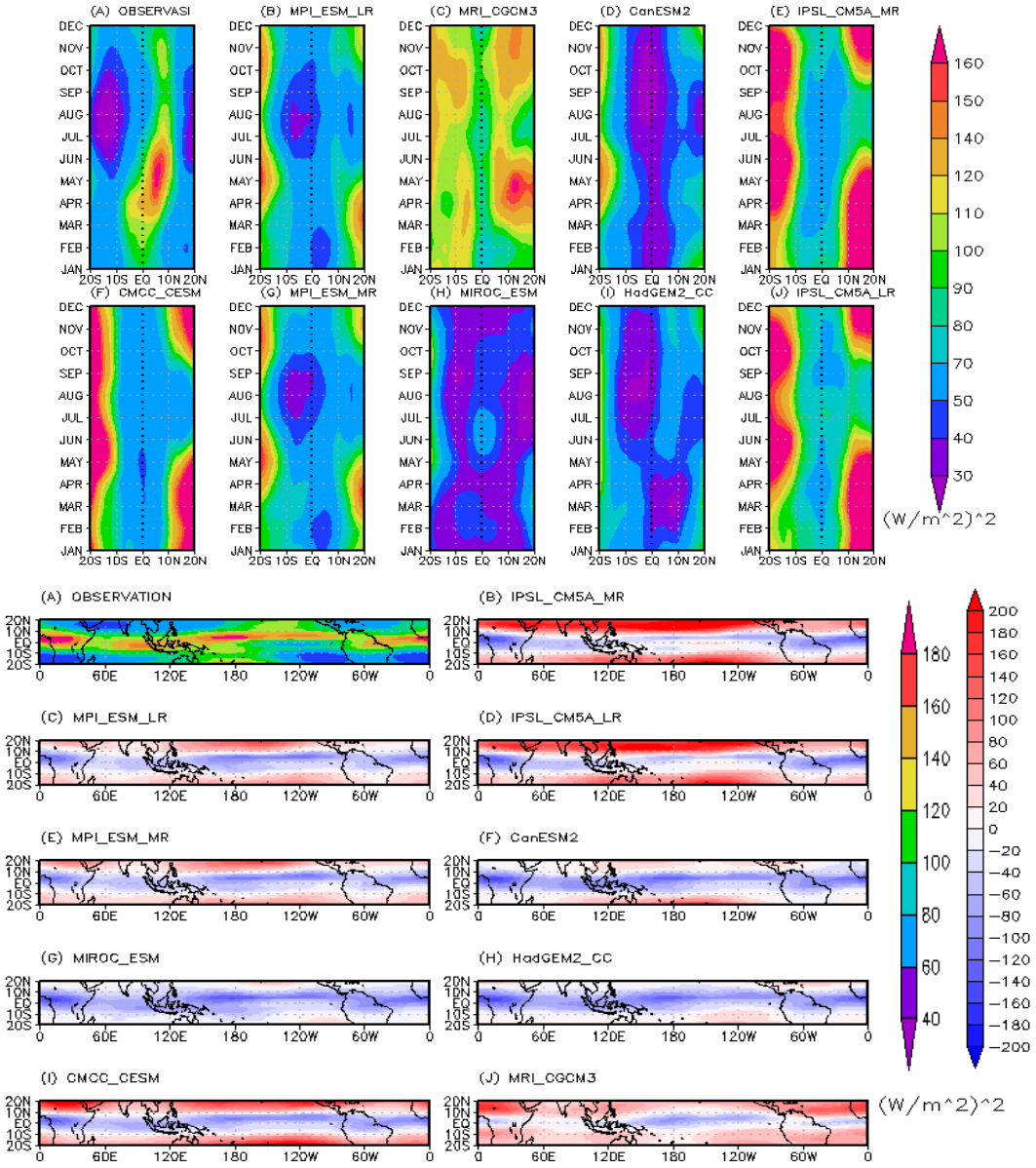

Figure 2. Seasonal cycle of Kelvin wave activity and its spatial distribution in JJA (June, July, August) from the observation (a) and CMIP5 models (b-j). The values in Figs. 2b-j (bottom) indicate residual values (model minus observation).

Figure 4 shows that seasonal cycle of ER waves as well as their spatial distributions in the observation and CMIP5 model simulations. The ER wave activity is observed from boreal spring to boreal winter (from December to April) with amplitude 130–150 $(W/m^2)^2$. The peak is observed in August. A secondary active period of ER wave appears in the SH, from January to March. The amplitude is much weaker compared to those in the observation, about 50 – 70 $(W/m^2)^2$. The CMIP5 models that exhibit a similar seasonal cycle of ER waves as in the observation are CanESM2, HadGEM2-CC, **I**PSL-CM5A-LR and IPSL-CM5A-MR. These models are able to simulate double peaks (in the NH and SH) of ER

wave seasonal cycle as in the observation, but with weaker amplitudes. Furthermore, focusing on the spatial distribution of ER waves, it is well established that the ER wave activity maximized over the northern and southern parts of the maritime continent [5].

In particular, the ER waves are strongly observed over the western north Pacific basin and along the Atlantic basin. Both IPSL-CM5A-MR and IPSL-CM5A-MR can mimic the spatial pattern of ER waves in JJA, but tend to be overestimate. In particular, the amplitude of ER waves is much stronger in the model around the ITCZ regions. In IPSL-CM5A-MR, the model also underestimates the amplitude of ER waves over the northwestern part of the tropical Pacific basin.

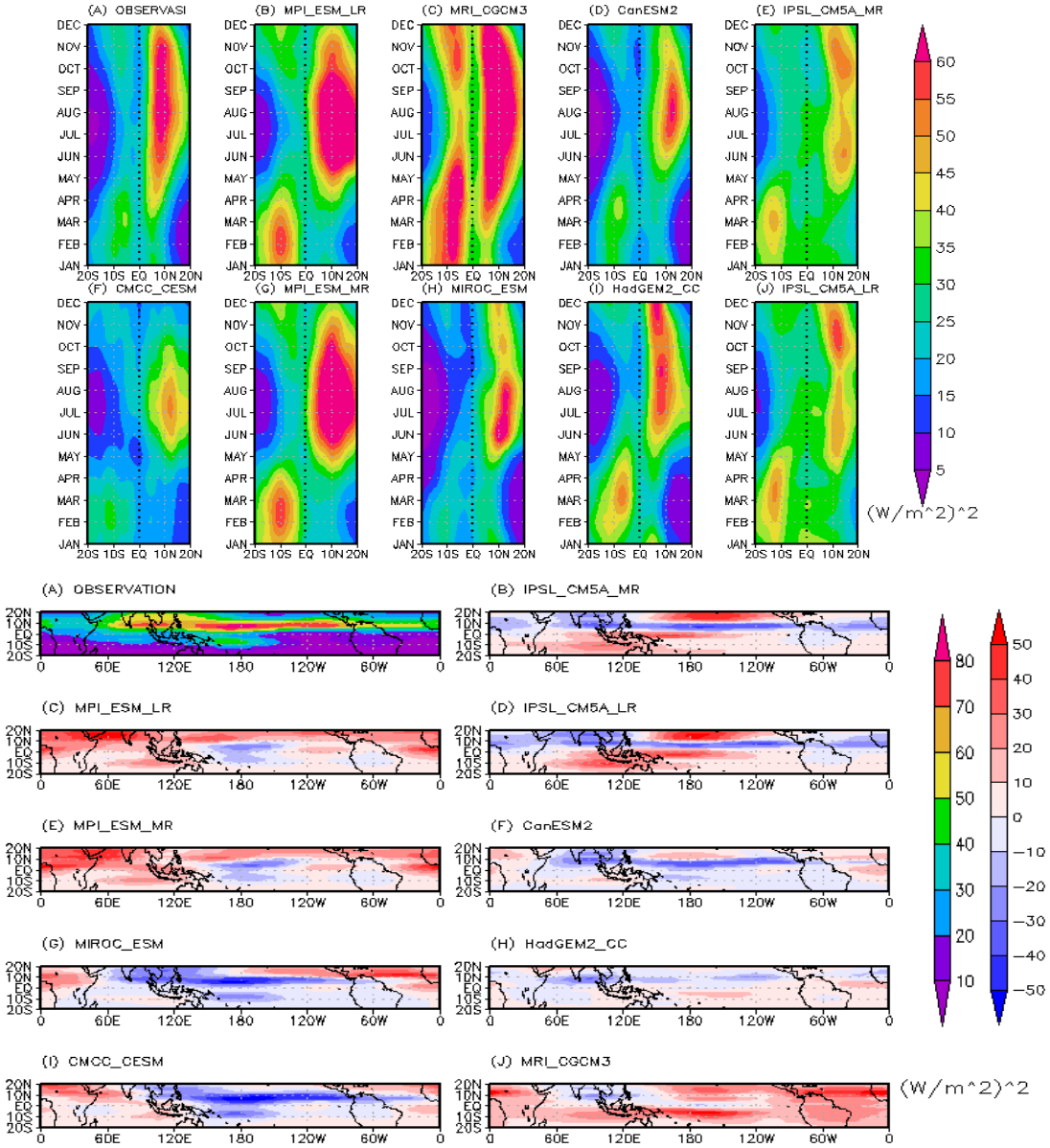

Figure 3. Seasonal cycle of MRG wave activity and its spatial distribution in JJA (June, July, August) from the observation (a) and CMIP5 models (b-j). (b-j). The values in Figs. 3b-j (bottom) indicate residual values (model minus observation).

Finally, the seasonal cycle of TD-type waves and their spatial distribution in the model and the high-top CMIP5 models are presented in Fig. 5. The TD-type waves, in general, have similar seasonal cycle as the ER waves. The MRG wave activity is strongly observed from boreal spring to boreal winter (from December to April) with amplitude 110–130 $(W/m^2)^2$, with the peak occurring in August. A secondary active period of TD-types waves are observed from January to March in the SH. These characteristics are consistent with the results found by Huang *et. al* 2013 and they argued that TD-type waves are intimately associated with the tropical cyclone (TC) geneses/activities. Furthermore, the high-top CMIP5 models that successfully represent the seasonal cycle of TD-type wave are CanESM2, IPSL-CM5A-MR, IPSL-CM5A-LR and HadGEM2-CC. These models are similar with the models that are able capturing the MRG wave activity, suggesting that the MRG and TD-type waves are interacting and/or coupled. These models, however, have lower amplitude compared to the observation than others.

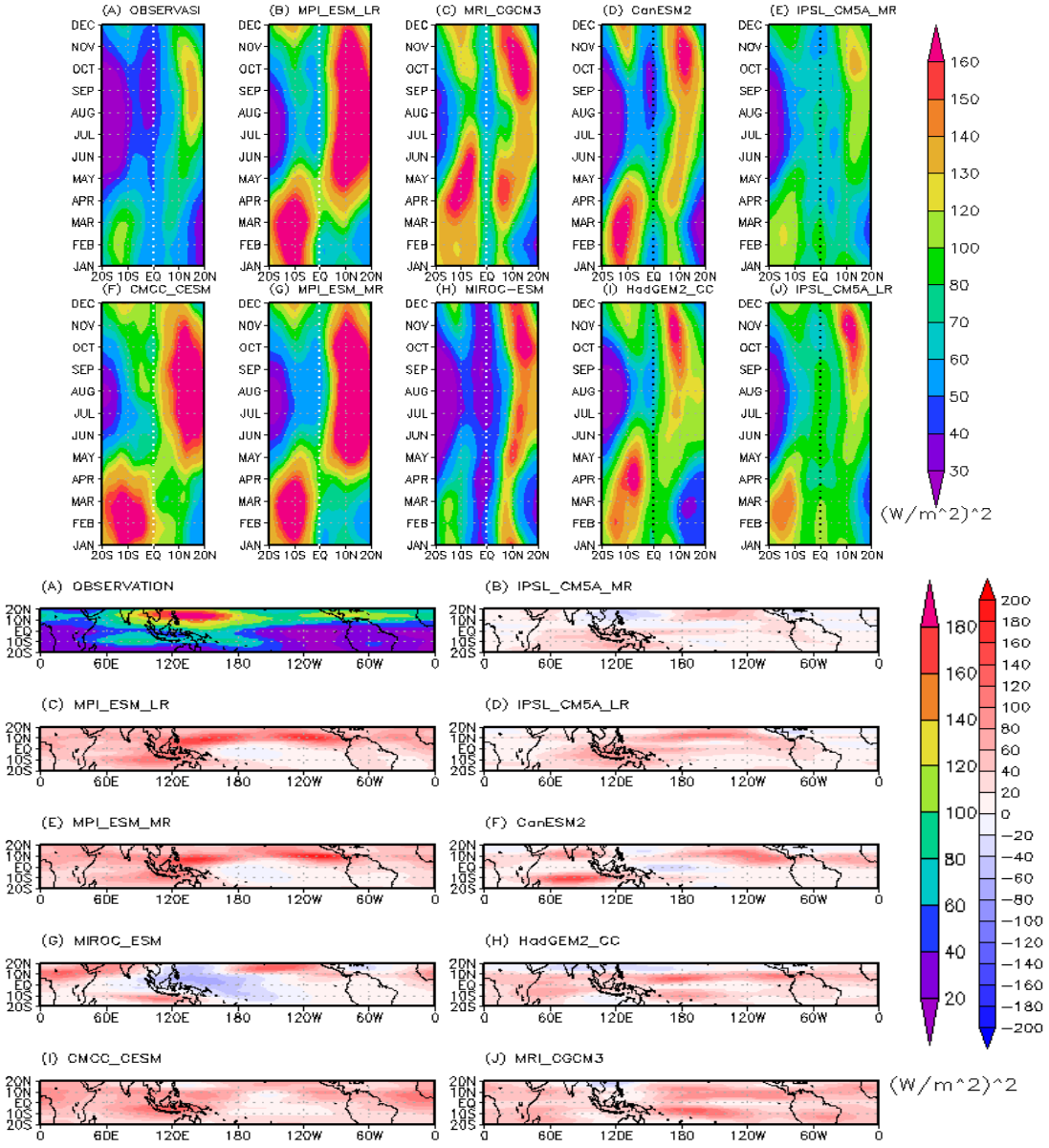

Figure 4. Seasonal cycle of ER wave activity and its spatial distribution in JJA (June, July, August) from the observation (a) and CMIP5 models (b-j). (b-j). The values in Figs. 2b-j (bottom) indicate residual values (model minus observation).

In terms of spatial distribution, there are two regions with strongest biases; firstly, the positive biases are observed over the Indian Ocean, central Pacific Ocean and Atlantic Ocean. Secondly, the negative bias (underrepresented amplitude of TD-type waves) are observed over the northwestern Pacific ocean, indicating that most high-top CMIP5 models still underestimate the frequency of TC activities compared to the observation.

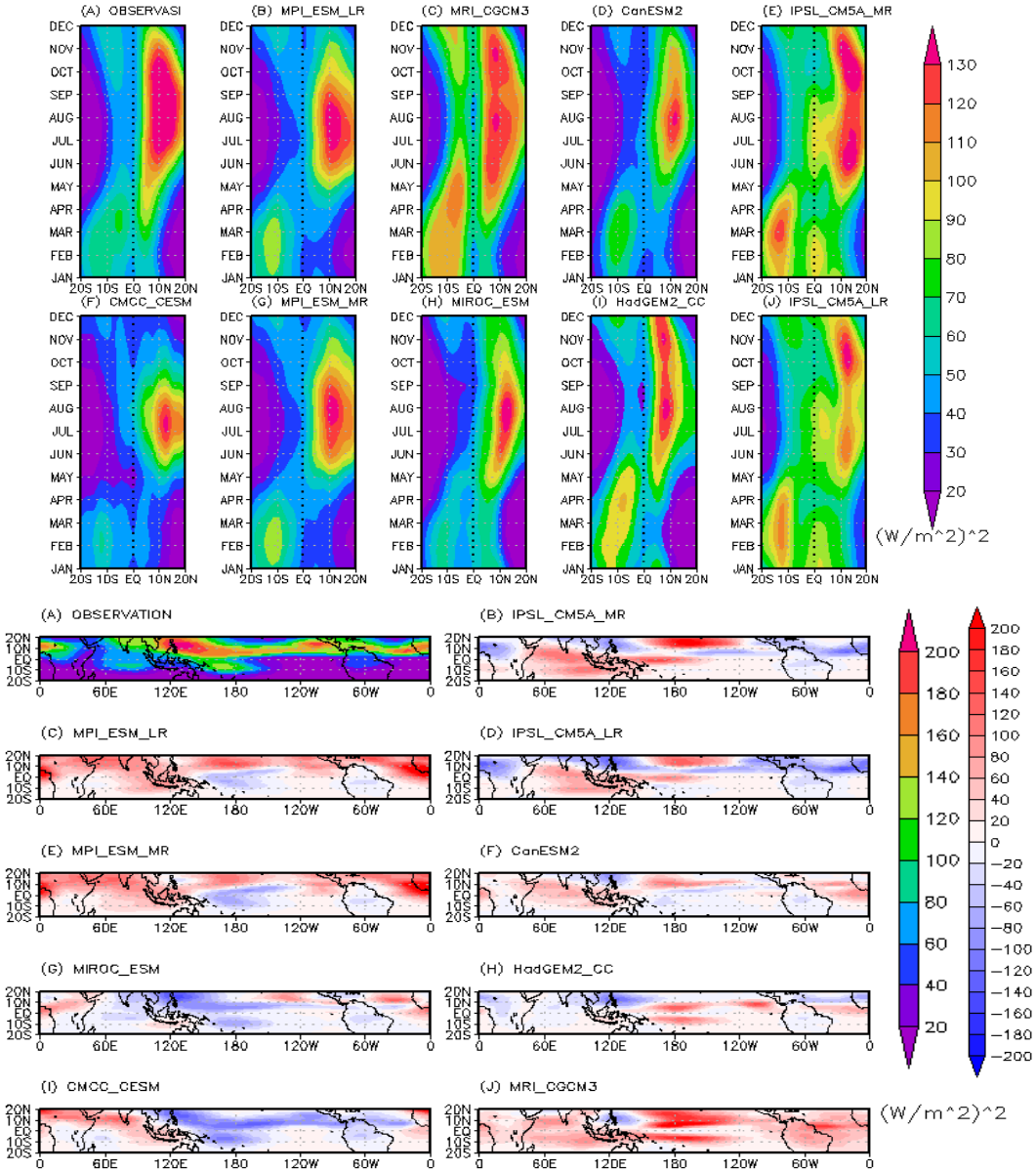

Figure 5. Seasonal cycle of TD-type wave activity and its spatial distribution in JJA (June, July, August) from the observation (a) and CMIP5 models (b-j).

According these result, model that can simulate CCEWs tend to have an intermediate complexity and resolution, such as IPSL, CanESM2 and HandGEM2-CC. We also aware that the types of the convective parameterization e.g., Convective Available Potential Energy (CAPE) used by the model will results in different CCEWs activity [4,13,14,1]. We found that model that has complex convective parameterization (rather than the simplified version) tend to better simulate the seasonal variability of

CCEWs. Further studies are required to understand the extent to which the convective parameterization affects the variability and amplitude of CCEWs in coupled GCM simulations.

4. Summary

This study evaluates some characteristics of CCEWs, including Kelvin waves, mixed Rossby-gravity waves, equatorial Rossby waves, and tropical depression (TD)-type waves, in some high-top CMIP5 models. The seasonal variability of each CCEW type was analyzed by using space-time spectral analysis (STSA). The key results of the current study are summarized as follow:

1) Most high-top CMIP5 models are capable in simulating CCEWs, as can be seen from the STSA analysis. The seasonal variability of Kelvin waves is well represented in MPI-ESM-LR and MPI-ESM-MR.

2) The seasonal variability of MRG waves is well simulated in CanESM2, HadGEM2-CC, IPSL-CM5A-LR and IPSL-CM5A-MR.

3) The seasonal variability of ER waves is well represented by CanESM2, HadGEM2-CC, IPSL-CM5A-LR and IPSL-CM5A-MR and maximized during boreal spring.

4) The seasonal variability of TD-type waves is well represented in CanESM2, HadGEM2-CC, PSL-CM5A-LR and IPSL-CM5A-MR, with maximum activity observed during boreal summer.

5) Our results indicate that the capability of CMIP5 models in representing seasonal variability of CCEWs highly depends on the convective (cumulus) parameterization and the resolution used by the models.

Further studies are required to understand what causes the discrepancies among the model simulations. We should note that without a realistic Kelvin wave and TD-type wave, the MJO and tropical cyclone (TC) genesis would not be able to be simulated in GCMs since the structure and propagation of the MJO and TC is similar to the convectively coupled Kelvin wave and TD-type waves.

Acknowledgment

We thank the reviewers for their constructive comments and WCRP for providing CMIP5 datasets.

References

[1] Alsepan G, Lubis S W, Setiawan S 2016 Analysis of the equatorial lower stratosphere Quasi-Biennial Oscillation (QBO) using ECMWF-Interim Reanalysis Data Set. *Earth Environ. Sci* 31 : 1-14.
[2] Fatullah N Z, Lubis S W and Setiawan S 2017 Characteristics of Kelvin waves and Mixed Rossby-Gravity waves in opposite QBO phases. *Journal IOPscince* doi.org/10.1088/1742-6596/755/1/011001
[3] Faturochman I, Lubis S W and Setiawan S 2017 Impact of Madden-Julian Oscillation (MJO) on global distribution of total water vapour and column ozone. *Journal IOP Science* doi.org/10.1088/1755-1315/54/1/012034.
[4] Lubis S W, Setiawan S 2010 Identification of Equatorial Atmospheric Kelvin Waves based on NCAP/NCAR Reanalysis I Data. Journal of Physics 12:71-82. ISSN 0854-3046.
[5] Lubis S W, Jacobi C 2015 The modulating influence of convectively coupled equatorial waves (CCEWs) on the variability of tropical precipitation. *J.Climtol*. **7**(35):1465-1483.

[6] Rakhman S, Lubis S W, Setiawan S 2017 Impact of ENSO seasonal variation of Kelvin wave and mixed Rossby-Gravitu waves. *Journal IOPscince*. doi:10.1088/1755-1315/54/1/012035.
[7] Flato G, J Marotzke, B Abiodun, P Braconnot, S C Chou, W Collins, P Cox, F Driouech, S Emori, V Eyring, C Forest, P Gleckler, E Guilyardi, C Jakob, V Kattsov, C Reason and M Rummukainen 2013. Overview: *Evaluation of Climate Model* In: Climate Change: The Physical Science Basis. Contribution of Working Group I to the Fifth Assessment Report of the Intergovernmental Panel on Climate Change 741-866.
[8] Takayabu Y N 1994 Large-scale cloud disturbances associated with equatorial waves. I:Spectral features of the cloud disturbances. *Journal of the Meteorological Society of Japan*. **72**(3):433–449.
[9] Kawatani Y, Takahashi M, Sato K, Alexander S P, Tsuda T 2009 Global distribution of atmospheric waves in the equatorial upper troposphere and lower stratosphere: AGCM simulation of sources and propagation. *J. Geophys. Res.* **114** doi: 10.1029/2008JD010374.
[10] Lot F, Denvil S, Butchart N, Cagnazzo C, Giorgetta M A, Hardiman S C, Manzini E, Krismer T, Duvel J P, Maury P, Scinocca J F, Watanabe S, Yukimoto S 2014 Kelvin and Rossby-gravity wave packets in the lower stratosphere of some high-top CMIP5 model. *Journal of Geophysical Research: Atmospheres.* doi:10.1002/2013JD020797.
[11] Tiedtke M 1989. A comprehensive mass flux scheme for cumulus parameterization in large-scale models. *Mon. Wea. Rev*. (117): 1779–1800.
[12] Emanuel K A 1991: A scheme for representing cumulus convection in large-scale models. *J. Atmos. Sci*. **48:**2313–2329.
[13] Kiladis G N, Matthew C, Wheeler, Patrick T, Katherine H, Straub, Paul E Roundy 2009 Convectively coupled equatorial waves. *Reviews of Geophysics*. **47**(2):1–42.
[14] Taylor K E, Stouffer R J, Meehl G. 2007 A Summary of the CMIP5 Experiment Design. World 1–33.
[15] Huang P, Chou C, Huang R 2013 The activity of convectively coupled equatorial waves in CMIP3 global climate models. *Theoretical and Applied Climatology*. 112(3–4): 697–71.
[16] Nordeng TE 1994 Extended versions of the convective parametrization scheme at ECMWF and their impact on the mean an transient activity of the model in the tropics. ECMWF Research Department Tech. European Centre for Medium-Range Weather Forecasts.
[17] Wheeler M, Kiladis G N 1999 Convectively coupled equatorial waves: analysis of cloud and temperature in the wavenumber-frequency dominan. *J Atmos Sci*. **56**(3):374-339.
[18] Wheeler M, Kiladis G N, Webster P J 2000 Large-scale dynamical fields associated with convectively coupled equatorial waves. *J Atmos Sci*. **57**(5): 613-640.
[19] Yang G Y, Hoskins B J, Slingo J M. 2011. Equatorial waves in opposite QBO phases. *J. Atmos. Sci.* **68**: 839–862, DOI: 10.1175/2010JAS3514.1.
[20] Zhang G J, McFarlane N A 1995 Sensitivity of climate simulations to the parameterization of cumulus convection in the Canadian Climate Centre general circulation model. Atmos-Ocean **33**(3):407–446.